# The nature of bonding in metal-metal singly bonded coinage metal dimers: Cu2 , Ag2 and Au2

Slavko Radenković, David Danovich, Sason Shaik, Philippe C. Hiberty, Benoît Braïda

## To cite this version:

Slavko Radenković, David Danovich, Sason Shaik, Philippe C. Hiberty, Benoît Braïda. The nature of bonding in metal-metal singly bonded coinage metal dimers: Cu2 , Ag2 and Au2 . Journal of Theoretical and Computational Chemistry, World Scientific Publishing, 2017, 10.1016/j.comptc.2017.02.013 . hal-01514930

**HAL Id: hal-01514930**

**https://hal.sorbonne-universite.fr/hal-01514930**

Submitted on 26 Apr 2017

**HAL** is a multi-disciplinary open access archive for the deposit and dissemination of scientific research documents, whether they are published or not. The documents may come from teaching and research institutions in France or abroad, or from public or private research centers.

L'archive ouverte pluridisciplinaire **HAL**, est destinée au dépôt et à la diffusion de documents scientifiques de niveau recherche, publiés ou non, émanant des établissements d'enseignement et de recherche français ou étrangers, des laboratoires publics ou privés.

# The Nature of Bonding in Metal-Metal Singly Bonded coinage metal dimers: $Cu_2$, $Ag_2$ and $Au_2$

*Slavko Radenković,[a,b] David Danovich[c], Sason Shaik[c], Philippe C. Hiberty[d] and Benoît Braïda*[,a]*

[a] Sorbonne Universités, UPMC Univ Paris 06, CNRS, Laboratoire de Chimie Théorique, cc 137 – 4,
place Jussieu F. 75252 PARIS CEDEX 05 – France

[b] Present address: University of Kragujevac, Faculty of Science, 34000 Kragujevac, Serbia

[c] Institute of Chemistry and The Lise Meitner-Minerva Center for Computational Quantum
Chemistry, Hebrew University of Jerusalem, 91904, Jerusalem, Israel

[d] Laboratoire de Chimie Physique, UMR CNRS 8000, Groupe Théosim, Université de Paris-Sud,
91405 Orsay Cédex, France

*Emails: slavkoradenkovic@kg.ac.rs, david.danovich@gmail.com, sason.shaik@gmail.com,
philippe.hiberty@u-psud.fr, benoit.braida@upmc.fr

**RECEIVED DATE ()**

**Title Running Head:**

**Abstract:**

The nature of the single bond in the three isoelectronic coinage metal dimers $Cu_2$, $Ag_2$ and $Au_2$ is investigated by means of the *ab initio* Breathing Orbital Valence Bond (BOVB) method, which allows one to calculate the respective contributions of the covalent and ionic structures to the total wave function, as well as the resonance energy arising from their mixing. It is shown that the BOVB method at its highest level provides bond dissociation energies in very good agreement with reference CCSD(T) values for the three dimers. It is also found that the covalent/ionic resonance energy is important in all three cases, contributing to 40-50% to the total bonding energy, thus qualifying the bonds in $Cu_2$ and $Au_2$ as quasi-charge-shift bonds, and that of $Ag_2$ as a borderline case in-between classical covalent bond and charge-shift one. These results are further confirmed by analyses of the wave functions in terms of the Atoms-in-Molecule theory, which show that the Laplacian of the density at the bond critical point is large and positive in all three cases, which classifies the three bonds as charge-shift bonds within this theory.

Keywords: Valence-Bond Theory, Hybridization, Non-Orthogonal Orbitals, Chemical bond, Charge Shift Bond, metal bonding.

## 1. Introduction

Ever since the landmark paper of Gilbert Lewis in 1916 [1], the nature of the chemical bond continues to be a central topic in chemistry, and one that inspires many theoretical studies. The bond and its properties are behind all the intrinsic properties of compounds, including the possible reactions that compounds may undergo. Among main group elements, two-electron bonds have been traditionally classified as either covalent or ionic [2], with a continuous spectrum of situations in-between the two extremes, which are well characterized and distinguished in the framework of Valence Bond (VB) theory, as well as by Quantum Chemical Topology methods such as "Atom-in-Molecules" (AIM) [3-5]. Covalent (or polar-covalent) bonding is formed by sharing two electrons between the two atoms; while ionic bonding is formed by transferring one electron from one atom to the other, and is stabilized by electrostatic attraction between the negative and positive charge centers. In the AIM framework, a covalent bond is characterized by a rather large value of the charge density, $\rho(r_c)$, at the bond critical point and a negative value of the Laplacian $\nabla^2\rho(r_c)$, whereas closed-shell interactions and ionic bonds in heteropolar compounds possess a low $\rho(r_c)$ and a positive Laplacian.

As a complement to the above description, recent modern VB studies [6-13] have shown that there exists a third class of electron-pair bonding, called charge-shift (CS) bonding. In VB theory, CS bonding is characterized by exceptionally large resonance energies associated with the mixing of the covalent and ionic components of the bond wave function. Thus, in CS bonds (CSBs), which may be homopolar as well as heteropolar, the resonance energy is the major component of the bonding energy, while covalent coupling and/or ionic attraction are of minor importance and in some notable cases are altogether repulsive, like in $F_2$ for which the purely covalent interaction is repulsive at all distances [6]. In the AIM approach, CSB in homopolar cases is most easily recognized as displaying unique features that were initially considered as exceptions in former interpretations [14]. Thus, on the one hand CS bonds display significant density $\rho(r_c)$ at the bond critical point, a feature of covalent bonds, and on the other hand the Laplacian is *positive*, a feature of closed-shell interactions and ionic bonds [9].

Within the main group element, the territory of CSB involves homopolar bonds of compact electronegative and/or lone-pair-rich elements, heteropolar bonds of these elements among themselves and with other atoms (for example, the metalloids, such as silicon and germanium [7]), no-density bonds [9], dative bonds[15] and hypercoordinated molecules.[16] More generally, CSB occurs whenever the bond in question is surrounded by large adjacent electron density, which creates strong Pauli repulsion pressure and as such weakens the covalent component of the bond [12,13,17]. This excessive exchange-repulsion pressure can be created by lone pairs adjacent to the bond, like, e.g., in bonds between halogens, oxygen-oxygen bonds, and so on, but also by groups surrounding the bridgehead bond as in [1.1.1]propellane and many other small-ring propellanes or cage-compounds [13]. As such, it has been suggested that first-row transition metals could also be prone to CS bonding, as the $3s^23p^6$ semi-core electron pairs might well play the same role in transition metals as lone pairs in main group elements [10, 11]. In accord, a study of M–H bonds, where M is a first-row transition metal, showed that the CS-resonance energy is quite significant and increases from left to right of the periodic table [18]. In higher rows, metal–metal bonds in some bimetallic complexes could well be CSBs, as in $M_2$(formamidinate)$_4$ complexes (M = Nb, Mo, Tc, Ru, Rh, Pd) where large positive values of $\nabla^2\rho(r_c)$ have been reported [19]. In the same line, an AIM Analysis of the bonding in Mo−Mo bonded dimolybdenum complexes showed $\rho(r_c)$ larger than 0.15 au while the Laplacian $\nabla^2\rho(r_c)$ larger than 0.34 au at the bond critical points of six out of the eight investigated molecules, revealing substantial, albeit not complete, CS character [20].

All these indices, suggestive of the possibility that CSB may show up in many bonds between transition metals, prompted us to perform an *ab initio* VB study of three prototype bimetallic single bonds with a completely filled *(n-1)*d shell, in the $Cu_2$, $Ag_2$ and $Au_2$ isoelectronic series. Indeed, VB is the most direct method to distinguish between classical covalent bonding and CS bonding, as it expresses the wave function in terms of VB structures and allows us to calculate the resonance energy arising from the mixing of ionic structures to the covalent one. As such, it provides the energetic contribution of this resonance energy to bonding which may be compared to the purely covalent contribution. Moreover, complementary analyses following the AIM approach will also be performed to compare with the VB results.

## 2. Computational details.

The equilibrium geometries of the studied molecules were optimized by means of the coupled cluster CCSD method using the Gaussian 09 program [21]. The LanL2TZ(f) basis set involving pseudopotentials [22] for the coinage metals, and the Dunning's correlation consistent polarized valence triple ζ basis set (cc-pVTZ) for H, F and Li atoms were employed. The reference values of the bond dissociation energies were obtained through the CCSD(T) single-point energy calculations. The AIM bond parameters were calculated based on the CCSD densities using the Multiwfn program [23]. The VB calculations were carried out with the XMVB 2.1 program [24]. The VBSCF and the different levels of BOVB methods used in this study have been described in details elsewhere [25,26].

## 3. Valence bond description and the nature of electron correlation in coinage metal dimers.

At first sight, bonding in the coinage metal dimers appears to be simple. In the corresponding atoms the valence shell, which includes *(n–1)*d and *n*s atomic orbitals (with $n$=4 for Cu, 5 for Ag and 6 for Au), is almost completely filled in their ground *(n–1)*$d^{10}$ *n*$s^1$ configuration. A simple electron-pair bond could thus be expected in the metal dimer ground states. Two molecules could be considered as second row singly bonded analogs of these dimers, either the $Li_2$ molecule, if the filled *(n–1)*$d^{10}$ shell in the coinage metals is considered inert and acting more like a "semi-core" ; or the $F_2$ molecule, if the *(n–1)*$d^{10}$ shell in the coinage metal act more like the lone pairs in fluorine. The nature of the *(n–1)*$d^{10}$ shell is thus the key that will determine the nature of bonding, standard covalent or charge-shift, in these systems. In classical VB theory, the 2c/2e bond in homo-atomic dimers is described by a mixing of a covalent and two symmetrically equivalent ionic structures (structures **1-3** in Figure 1). They correspond to the three different possible ways of distributing and singlet-coupling two electrons in two active orbitals. The usual convention in graphical representation of classical VB structures is used, with the line connecting the two dots in structure **1** indicating the singlet coupling between the two electrons (then represented by two dots) in the two (active) orbitals. As always in classical VB methods the active orbitals are constrained to remain strictly localized, at variance with MO theory based methods, but also at variance with the semi-localized family of VB methods such as GVB and Spin-Coupled VB [26].

For the sake of simplicity, pure s-type atomic orbitals (AOs) drawings are displayed in Figure 1 for structures **1**–**3** (and pure p-type AOs for structures **4**–**9**), but because an extended basis set is used in the calculations these orbitals can of course polarize at will (computed VB orbitals will be shown in the following). In practice, the *n*s active orbitals come out to be of predominantly s character in the optimized VB wave functions. Therefore, the coinage metal dimers look closer to the prototype $H_2$ and $Li_2$ molecules, with a 2c/2e bond established between orbitals of predominantly *n*s AOs types, leaving the *n*p functions basically unoccupied. However, it is well known from MO theory that, to get a quantitative value for the bond dissociation energy in $H_2$ and $Li_2$, configurations featuring double excitations from the *n*s to the *n*p orbitals have to be incorporated into the ground state wave function. In VB theory, this corresponds to the inclusion of the π bonding type of structures **4**–**9** depicted in Figure 1. In the case of $Li_2$, the contribution of the π bonding structures amounts to about 10 kcal/mol, that is close to 50% of the bonding energy (using the cc-pVTZ basis set), and their contribution is a bit smaller but still substantial in the BDE of the $H_2$ molecule. It is thus expected that these structures would also be requested to obtain a quantitative value for the bond dissociation energy for the coinage metal dimers.

---- insert Figure 1 near here ----

Table 1 displays the bond dissociation energy (BDE) at different levels of Valence Bond theory along with CCSD(T) data in the same basis set, and experimental bond dissociation energies as references. The M–M distances used both in all the VB and CCSD(T) calculations are those optimized at the CCSD level using the same basis set and pseudopotential, and are 2.325 Å, 2.621 Å and 2.518 Å respectively for $Cu_2$, $Ag_2$, and $Au_2$. These bond lengths are slightly longer than the experimental bond distances by less than 0.1 Å for $Cu_2$ and $Ag_2$, and by less than 0.05 Å for $Au_2$. As the BDE are concerned, the agreement of CCSD(T) with the experimental reference value is also reasonably good and sufficient for this study. The reasonable accuracy of both CCSD bond distances and BDE as compared with experiment validates our choice of basis set and associated pseudopotential.

--- insert Table 1 near here ---

Let us proceed with the Valence Bond results in Table 1. The first entries allow us to assess the impact on the BDE of including the π-type structures for the dimers. These structures increase the bond dissociation energy by more than 7 kcal/mol for the copper dimer, which is just a bit smaller than what is found for the reference $Li_2$ dimer. The improvement of the BDE is smaller but still substantial, about 4 kcal/mol, for the other lower-row metal dimers.

Let us mention that a more extended selection of structures has also been tested that includes *(n–1)*d orbitals into the active space, and features some d-d bonding. These structures could be considered as arising from the interaction of two metal atoms in the first atomic excited state of $(n-1)d^9ns^2$ configuration, such atomic excited state lying not sky-high in energy relative to the ground state. However, inclusion of more structures of this type has lead to a very marginal improvement of the BDEs, and thus the basis of 9 structures depicted in Figure 1 is selected for the BOVB calculations.

The L-BOVB wave function differs from the L-VBSCF one by the fact that the different VB structures have their own and specific sets of orbitals. The "L" indicates that the inactive electron pairs remain strictly localized on a specific atom (or fragment), while the "BO" acronym refers to "Breathing Orbitals". The orbital sets are optimized (together with the structure coefficients) in the presence of each other, and thus they achieve a compromise between adaptation to the mean field of their specific structures and optimal resonance between the different structures. The VBSCF method is the standard *ab initio* classical VB method that includes static electron correlation, while the L-BOVB method includes part of the dynamical correlation that has been coined as "Breathing Orbital effect", and belongs to the type of correlation that is also called in the MO community "orbital relaxation effect". Let us remark that the L-VBSCF and L-BOVB wave functions are identical at dissociation limit for 2c/2e bonded systems and correspond to uncorrelated separate atoms, and therefore the improvement in BDE that is obtained when introducing this "breathing orbital effect" comes from what could be called the *differential orbital relaxation effect*, i.e. the amount of this specific part of dynamical correlation that changes when going from dissociation limit to equilibrium. This effect is particularly large in cases where there is a strong interplay between the active and inactive electrons, and that includes the CSB systems. In the extreme case of the $F_2$ molecule, a complete charge-shift bond, the lone pair electrons relax strongly when the active electrons change from one configuration (covalent or ionic) to another, and the BDE is improved in this case by no less than 22.2 kcal/mol (more than the half of the final BDE at the highest BOVB level) as compared with the L-VBSCF level. This "breathing orbital" effect is usually much less important or even marginal in standard polar-covalent bonds with $Li_2$ or $H_2$ being the extreme opposite cases where the BDE is improved by less than 1 kcal/mol at the L-BOVB level. For the three metal dimers, the differential orbital relaxation effects can be quantified by taking the differences between the BDEs displayed in lines 2 and 3 in Table 1, and it amounts to a moderate value of 4.5 and 4.8 kcal/mol for $Cu_2$ and $Ag_2$ respectively, but to a much larger amount of 13.7 kcal/mol for $Au_2$. These quantities correspond to the relaxation effect of the *(n–1)*d electrons when the *n*s electrons change from one configuration (covalent or one of the two ionics) to another, and thus can be considered as a "cross correlation" between the *(n–1)*d and the *n*s shells. It is not very surprising that this "BO effect" is larger in the case of $Au_2$, because, due to relativistic effects, both the radii and energies of the *(n–1)*d and *n*s orbitals are closer in the case of gold than in the lighter coinage metals, therefore a larger "cross-correlation" in this case.

--- insert Figure 2 near here ---

In the second level of the BOVB method, i.e. the SL-BOVB level, some further dynamical correlation is included into the wave function by "splitting" ("S") one of the electron pairs, i.e. going from a description with the two electrons of the pair that doubly occupy the *same* orbital strictly localized on one of the two center, to a description with two singlet coupled electrons in *two different* orbitals, still both strictly localized on the *same* center (at variance with a covalent coupling). This is schematically illustrated in Figure 2, where the new "split" ionic structures **2'** and **3'** replaces in the SL-BOVB wave function the original ionic structures **2** and **3**. This orbital "splitting" mimics the radial and angular correlation of a *specific electron pair*, which in MO-CI methods could be introduced alternatively through double excitations, or using an explicit correlation function such as a Jastrow factor [30]. In $Ag_2$ and $Au_2$, the 4s pairs in the main ionic structures are split, as cartooned in Figure 2. The computed 4s-type orbitals at the SL-BOVB level for $Au_2$ are also displayed in Figure 3. As can be seen, the splitting of the 4s-type orbital in the ionic structure **2'** provides after optimization a pair or hybrid orbitals that point in opposite directions, principally mimicking what is usually called angular correlation effect. The inclusion of this "S" effect in the BOVB wave-function, although having a significant consequence on the shapes of the corresponding orbitals, leads to variable improvements of the BDE, as can be seen from the values displayed in entry 4 of Table 1 when compared with the previous line (L-BOVB entry). In the case of $Cu_2$, the splitting of the 4s-type orbitals only leads to a marginal improvement in BDE, and thus in this molecule we have therefore used a split $3dz^2$ pair in the main covalent structure **1**, thus introducing instead some dynamical correlation in the 3d shell. This choice was motivated by two reasons: first by the fact that we suspected a strong *differential* dynamical correlation effect coming from the 3d shell itself in $Cu_2$, and second because the VB orbitals that intend to describe the $3dz^2$ pairs span the same subset of basis functions (s, $p_z$ and $d_{z^2}$ type) as the so-called "4s-type" VB orbitals. With this choice, the BDE of the copper dimer comes out to be significantly improved by some 6.0 kcal/mol as compared with the L-BOVB level. This correlation effect is expected to be smaller in $Ag_2$ and even more in $Au_2$, because the *(n-1)*$dz^2$ orbital radii decrease from gold to silver and from silver to copper, and the more compact the electron pair the larger its correlation. Splitting the $4dz^2$ (resp. $5dz^2$) orbital pair has nevertheless been tested in the silver and gold dimer, and lead to smaller improvement in the BDE than the original splitting of the "*n*s pairs, and thus this latter choice has been retained. Note also that despite the so-called *(n-1)*$dz^2$ and *n*s types of VB orbitals span the same subset of basis functions, they both retain their original character in the optimized SL-BOVB wave functions whichever orbitals are split: the so-called "*(n-1)*$dz^2$" optimized VB orbitals come out with small coefficients on s (and $p_z$) type of basis functions, and likewise the "*n*s" VB orbitals emerge with small coefficients on $dz^2$ (and $p_z$) type of basis functions.

--- insert Figure 3 near here ---

The highest level of theory of the BOVB method is the SD-BOVB level. As compared with the SL-BOVB level, the inactive electron pairs (those that are described by a single doubly occupied orbital in *all* the structures) are now allowed to delocalize onto the other center. This is simply obtained by allowing these orbitals to span the whole basis of functions corresponding to their irreducible representation in the $D_{\infty h}$ group, instead of restricting them to span only a subset of those basis functions that are centered on the same atom. The active orbitals (which only include the 4s-type orbitals in $Ag_2$ and $Au_2$, but also the $3dz^2$-type orbitals in $Cu_2$) are frozen in the optimization of the SD-BOVB wave function, and thus remain unchanged relative to the SL-BOVB level. This standard procedure serves to avoid potential instabilities coming from orbital flipping between active and inactive orbitals when some of them have basis functions in common. This "D" option has the effect of reducing the Pauli exchange repulsion between the inactive doubly occupied orbitals (e.g. lone pairs), owing to the additional flexibility of the BOVB wave function. For example, this "D" effect improves the BDE of the $F_2$ molecule by 4.3 kcal/mol in the cc-pVTZ basis set. As the metal dimers are concerned (last line in Table 1), the BDE are much improved for $Cu_2$ and $Au_2$ at the SD-BOVB level, by 8.0 and 7.8 kcal/mol respectively when compared with the SL-BOVB level, i.e. it is almost two times larger than in the $F_2$ molecule. The improvement is significantly smaller (2.6

kcal/mol only) for the silver dimer. This is in line with the trend in bond distances among the metal dimer series, which itself is largely connected to the size of the bonding *n*s orbitals: the 5s orbital in silver has a larger spatial extent than the 4s in copper, leading to a longer bond length, therefore a smaller repulsion between the *(n–1)*d shells of the two atoms, and as a result a smaller "D effect" in the silver dimer. By contrast, the 6s orbital in gold has a smaller spatial extent due to the strong relativistic effects, therefore the bond distance is shorter in $Au_2$ than in $Ag_2$, and thus the repulsion between the 5d shells (which shrink due to the relativistic effect but to a much smaller extent than the 6s orbitals) makes the "D effect" large again.

Overall, the large difference in the bond dissociation energy at the L-VBSCF vs. SD-BOVB reveals the very large differential dynamical correlation (ddc) effect in the copper and gold dimers, respectively of 18.5 and 23.5 kcal/mol, coming from the (*n–1*)d shell and from the cross correlation between the (*n–1*)d and ns shells. When compared with the second row homonuclear dimers, the ddc is not as large as in the $F_2$ dimer where it amounts to more than 30 kcal/mol overall (cc-pVTZ basis set), but it is way larger than in the $Li_2$ dimer (3.4 kcal/mol only in the same basis set). Last, the ddc is smaller in $Ag_2$, with only 9.6 kcal/mol. As CSB is usually associated with large ddc,[31] the large ddc in $Cu_2$ and $Au_2$ are indicative of CSB character, which will be examined in the next section using adequate methods for probing the nature of bonding in these molecules.

Last, the final BDE that are obtained at the highest SD-BOVB level are in good to very good agreement with the reference CCSD(T) values computed in the same basis set, showing that despite using a very compact wave function (9 structures only), the SD-BOVB method is capable to recover the most significant part of the electronic correlation effect in these metal dimers, and thus could be safely used in the following to analyze in more details the nature of bonding in these molecules.

## 4. Charge-Shift Bonding character.

The Charge-Shift Bonding (CSB) concept originates from VB theory,[6,10,11] and has been defined as a bonding type where the major part of the bond dissociation energy comes from *resonance energy stabilization* between structures. In the case of 2c/2e bonded systems, that are described within classical VB theory by a mixing of covalent and ionic structures, the key quantity to characterize the bonding type is the "Charge Shift resonance energy" ($RE_{CS}$). It is defined, in cases where the covalent structure is the major one, as the resonance stabilization brought by the two ionic structures when mixed to the covalent structures, equation (1), where $E_{cov}$ and $E_{full}$ are the energies of the VB wave functions containing only the covalent structure(s) and the full (covalent plus ionic) basis of structures respectively.

$$RE_{CS} = E_{cov} - E_{full} \quad (1)$$

Let us note that even though in extreme cases such as $F_2$ the mixing of the ionic structures considerably stabilizes the wave function, providing a $RE_{CS}$ quantity that largely exceeds the total

BDE,[10] in all homonuclear CSB cases which we characterized so far, the full three-structure VB wave functions has ionic weights which are smaller than the weight of the covalent structure. Besides, the covalent vs. ionic ratio found in singly bonded systems made of two identical fragments appear to be basically constant in a given row of the periodic table, whatever the bonding nature (covalent, complete CSB, intermediate cases), a feature which has been rationalized [32]. Hence, the composition of the VB wave function in terms of covalent/ionic ratio does not enable one to characterize a bond as either of (polar-)covalent of CSB type, but it is the $RE_{CS}$, an energetic quantity, that allows such classification.

---- insert Table 2 near here ---

The SD-BOVB Chirgwin-Coulson weights [26,33] of the coinage metal dimers are displayed in Table 2, and they do not depart from this general empirical rule. The covalent structure is largely dominant with more nearly 84% weight in the copper dimer, typical of a single bond between identical first row atoms, while the ionic contribution increases in lower-row dimers, with a covalent structure that still remains the major one, though having a weight below 60% in the case of $Au_2$. This increase of the ionic structures weight when going down in a given column of the periodic table has been found also in dihalogen dimers in the past, with a covalent vs. ionic ratio similar to what is reported here for the coinage metal dimers. Remarkably, the weights of the π-type structures **4-9** are marginal despite a significant influence on the energies, indicating that these structures are not fundamental valence structures such as **1**-**3**, but their purpose is rather to bring some correlation (or dispersion) to the wave function.

In classical VB theory, the standard reference for a polar-covalent bond is a wave function that incorporates only Heitler-London-Slater-Pauling (HLSP) types of function built on strictly localized atomic-like orbitals [34], i.e. overall singlet functions that are more casually called "covalent structures". In the case of coinage metal dimers, a reference VB wave function $\psi_{cov}$ would thus include a combination of structures **1**, **4** and **5** only, while the total VB wave function $\psi_{full}$ would include the complete basis of 9 structures. In this study both wave functions have been computed at the SD-BOVB level in two different separate wave function optimizations, and the corresponding variational energies will be referred to as $E_{cov}$ and $E_{full}$ respectively in the following. Both $\psi_{cov}$ and $\psi_{full}$ dissociate to the same limit at the SD-BOVB level because the ionic structures vanish at long distances, and the common energy at dissociation limit will be referred to as $E_{diss}$. The $RE_{CS}$ in Table 3 has then been computed using equation (1), and the $D_{cov}$, $BDE$ and $\%RE_{CS}$ using equations (2), (3) and (4).

$$D_{cov} = E_{diss} — E_{cov} \quad (2)$$

$$BDE = E_{diss} — E_{full} \quad (3)$$

$$\%RE_{CS} = \frac{RE_{CS}}{BDE} \times 100 \quad (4)$$

A continuum of values exists for $\%RE_{CS}$ in 2c/2e bonds, ranging from close to 0% ($Na_2$ case [10]) to much over 100% ($F_2$ case[10]). It has originally been proposed to classify as CSBs all bonds where $\%RE_{CS}$ exceeds 50%, and the extreme cases where $RE_{CS}$ is fully responsible for bonding (where $\%RE_{CS}$ exceeds 100%) has been coined as "complete Charge Shift Bonds"[35].

---- insert Table 3 near here ---

In Table 3 various quantities characteristic of the nature of the chemical bond, covalent vs. CSB type, are gathered. Let us focus on the VB related data first. The covalent bonding energy, $D_{cov}$, varies like the total BDE: it decreases from $Cu_2$ to $Ag_2$, and then increases again reaching a maximum for $Au_2$. Therefore, the $RE_{CS}$ and $\%RE_{CS}$ quantities vary in the same direction. All three bonds unveil significant CSB character though, with substantially large $RE_{CS}$ in the three cases. As a formal characterization in terms of bonding type, both copper and gold dimer could be qualified as quasi-charge-shift bonds, with a $\%RE_{CS}$ very close to the 50% threshold, while the $\%RE_{CS}$ of the silver dimer being farther away from this limit appears as a borderline case. However, all three $\%RE_{CS}$ values are close enough to 50% so that the conclusions might arguably be considered as potentially affected by the accuracy of the methodology used, and it would thus be welcome to have a second verdict from a different theory to more clearly settle the issue at hand, and AIM theory can offer this possibility.

---- insert Figure 4 near here ---

Within AIM theory, the covalent and charge shift bonds in homopolar dimers are characterized through the sign of the Laplacian of the density at the bond critical point, $\nabla^2\rho(r_c)$: when negative it indicates a covalent bond, when positive a charge shift bond, the density at bond critical point $\rho(r_c)$ itself being non-negligible in both type of bonds. The values of $\rho(r_c)$ and $\nabla^2\rho(r_c)$ for the three coinage metal dimers, along with reference values for $H_2$, $Li_2$ and $F_2$, are displayed in the last two columns of Table 3. It should be noted that these quantities have been obtained from CCSD computed densities, thus from a completely different theory than the VB related quantities shown in Table 3. In all three coinage metal dimers, $\nabla^2\rho(r_c)$, despite being smaller than in the extreme case of difluorine, is clearly both significant and positive, and thus should qualify the bonds as CSBs from the AIM perspective. To have a more complete picture, 2D cuts of the distribution of $\nabla^2\rho(r_c)$ are displayed in Figure 4. The blue lines indicate positive values of $\nabla^2\rho(r_c)$, while the red lines correspond to negative values of $\nabla^2\rho(r_c)$. It is very clear at first sight that the distributions of $\nabla^2\rho(r_c)$ for the three coinage metal dimers are similar to those reported for the $F_2$ case, with negative values of $\nabla^2\rho(r_c)$ concentrated in a small region around each of the atoms, and positive values of $\nabla^2\rho(r_c)$ elsewhere, and in particular between the two atoms. By contrast, the picture is totally different in the case of the prototype covalent dimers $H_2$ and $Li_2$, which both display a large region of *negative* values of $\nabla^2\rho(r_c)$ *between* the two atoms. All in all, AIM theory unambiguously classifies the three coinage metal dimers as CSBs.

## 5. Conclusion.

The analysis and understanding of the nature of bonding in transition metal (TM) containing molecules is a key topic in modern molecular (bio)chemistry, as many (bio)chemical reactions and systems involve one or several metals. Metallic bonding has its own specific features, and is usually more challenging than bonding between main group atoms. The reason is the presence of two very different valence shells, the *(n-1)*d and *n*s shells, that have different spatial extensions and energies, can be partially filled depending on the metal and its oxidations sate, and usually involve a larger number of valence electrons than main group elements. Therefore, all these ingredients imply substantial correlation effects, often involving a combination of different types of correlation, which in return require an adequate and elaborate theoretical treatment. *Ab initio* classical Valence Bond theory has largely remained on the sidelines of this very large and important area of chemistry, with very limited studies of TM-containing systems so far. This is due both to the above-mentioned difficulties, but also for long because of computational limitations mainly coming from the very tough challenge of dealing with non-orthogonal orbitals. Such limitations are now over.

This article presents the first *ab initio* classical VB study of metal-metal bonding, in the homo-atomic dimers of coinage metals. These atoms are electron-rich with almost totally filled valence shells, and electron-pair bonding occurs in their electronic ground state mainly through interaction between singly occupied orbitals of *n*s type. The BOVB method at its best SD-BOVB level leads to Bond Dissociation Energies (BDE) that are in good agreement with reference CCSD(T) computed values using the same pseudopotential and basis sets. Correlation of the *n*s bonding electrons with inclusion of π-type structures involving *n*p atomic like orbitals, dynamic correlation of the *(n-1)*d electrons, and *(n-1)*d / *n*s cross-correlation, all needed to be incorporated into the wave function to obtain quantitative results. The SD-BOVB method has proved to be elegantly and efficiently capable of doing so, while at the same time keeping an extremely compact wave function (9 structures only).

As the nature of bonding is concerned, SD-BOVB results, with Charge Shift Resonance Energies ($RE_{CS}$) that amount to about ~50% of the total BDE for $Cu_2$ and $Au_2$ classifies these two dimers as quasi-charge-shift bonds, and with ~40% the $Ag_2$ dimers comes out as a borderline case. AIM theory on its side qualifies the three dimers as CSB. Hence, the filled *(n-1)*d shell in coinage metals acts to some extent as the lone pairs of $F_2$ to generate a substantial Charge Shift Bonding character in the dimers, albeit to a lesser extent.

These results are very encouraging for VB theory, and prompt us to explore more extensively the area of metallic systems where VB theory may be a valuable tool to improve our general understanding of bonding with and between transition metals. Very recent and major breakthrough in algorithms [36], combined with advanced and efficient recent implementations [24], now allow *ab initio* classical VB to take up the challenge.

## References

[1] G.N. Lewis, The atom and the molecule, J. Am. Chem. Soc. 38 (1916) 762-785.

[2] L. Pauling, The Nature of the Chemical Bond, third ed., Cornell University Press, Ithaca, New York, 1960.

[3] R.F.W. Bader, Atoms in Molecules: A Quantum Theory, Oxford University Press, Oxford, 1990.

[4] R.F.W. Bader, A quantum theory of molecular structure and its applications, Chem. Rev. 91 (1991) 893-928.

[5] R.F.W. Bader, Comment on the comparative use of the electron density and its Laplacian, Chem. Eur. J. 12 (2006) 7769-7772.

[6] (a) G. Sini, P. Maitre, P.C. Hiberty, S. Shaik, Covalent, ionic and resonating single bonds, J. Mol. Struct. Theochem 229 (1991) 163-169. (b) S. Shaik, P. Maitre, G. Sini, P. C. Hiberty, The charge-shift bonding concept. Electron-pair bonds with very large ionic-covalent resonance energies, J. Am. Chem. Soc. 114 (1992) 7861-7866.

[7] A. Shurki, P.C. Hiberty, S. Shaik, Charge-shift bonding in group IVB halides: A valence bond study of $MH_3$-Cl (M = C, Si, Ge, Sn, Pb) molecules, J. Am. Chem. Soc. 121 (1999) 822-834.

[8] S. Shaik, D. Danovich, B. Silvi, D.L. Lauvergnat, P.C. Hiberty, Charge-shift bonding - A class of electron-pair bonds that emerges from valence bond theory and is supported by the electron localization function approach, Chem. Eur. J. 11 (2005) 6358-6371.

[9] L. Zhang, F. Ying, W. Wu, P.C. Hiberty, S. Shaik, Topology of electron charge density for chemical bond from valence bond theory: A probe of bonding types, Chem. Eur. J. 15 (2009) 2979-2989.

[10] S. Shaik, D. Danovich, W. Wu, P.C. Hiberty, Charge-shift bonding and its manifestations in chemistry, Nat. Chem. 1 (2009) 443-449.

[11] S. Shaik, D. Danovich, B. Braida, W. Wu, P.C. Hiberty, New landscape of electron-pair bonding: covalent, ionic, and charge-shift bonds, in: D.M.P. Mingos (Ed.), The Chemical Bond II, Springer International Publishing, Cham, 2016: pp. 169–211.

[12] W. Wu, J. Gu, J. Song, S. Shaik, P.C. Hiberty, The inverted bond in [1.1.1]propellane is a charge-shift bond, Angew. Chem. Int. Ed. 48 (2009) 1407-1410.

[13] S. Shaik, Z. Chen, W. Wu, A. Stanger, D. Danovich, P.C. Hiberty, An excursion from normal to inverted C-C bonds shows a clear demarcation between covalent and charge-

shift bonds, ChemPhysChem 10 (2009) 2658-2669.

[14] L. Rincon, R. Almeida, On the topology of the electron charge density at the bond critical point of the electron-pair bond, J. Phys. Chem. A 102 (1998) 9244-9254.

[15] A.A. Fiorillo, J.M. Galbraith, A valence bond description of coordinate covalent bonding, J. Phys. Chem. A 108 (2004) 5126-5130.

[16] (a) B. Braida, P. C. Hiberty, The essential role of charge-shift bonding in hypervalent prototype $XeF_2$, Nature Chem. 5 (2013) 417-422. (b) B. Braida, T. Ribeyre, P. C. Hiberty A Valence Bond Model for Electron-Rich Hypervalent Species: Application to $SF_n$ (n=1, 2, 4), $PF_5$, and $ClF_3$, Chem. Eur. J. 20 (2014) 9643-9649. (c) B. Braida, P. C. Hiberty, Application of the Valence Bond Mixing Configuration Diagrams to Hypervalency in Trihalide Anions: A Challenge to the Rundle-Pimentel Model**,** J. Phys. Chem. A 112 (2008) 13045-13052.

[17] P. C. Hiberty, R. Ramozzi, L. Song, W. Wu, S. Shaik, The physical origin of large covalent-ionic resonance energies in some two-electron bonds, Faraday Discuss. 135 (2007) 261-272.

[18] J. M. Galbraith, A. Shurki, S. Shaik, A valence bond study of the bonding in first row transition metal hydride cations: What energetic role does covalency play? J. Phys. Chem. A 104 (2000) 1262-1270.

[19] R. Llusar, A. Beltran, J. Andres, F. Fuster, B. Silvi, Topological analysis of multiple metal-metal bonds in dimers of the $M_2$(formamidinate)$_4$ type with M = Nb, Mo, Tc, Ru, Rh, and Pd, J. Phys. Chem. A 105 (2001) 9460-9466.

[20] J.F. van der Maelen, J.A. Cabeza, QTAIM analysis of the bonding in Mo−Mo bonded dimolybdenum complexes, Inorg. Chem. 51 (2012) 7384-7391.

[21] Gaussian 09, Revision B.01, M.J. Frisch, G.W. Trucks, H.B. Schlegel, G.E. Scuseria, M.A. Robb, J.R. Cheeseman, G. Scalmani, V. Barone, B. Mennucci, G.A. Petersson, H. Nakatsuji, M. Caricato, X. Li, H.P. Hratchian, A.F. Izmaylov, J. Bloino, G. Zheng, J.L. Sonnenberg, M. Hada, M. Ehara, K. Toyota, R. Fukuda, J. Hasegawa, M. Ishida, T. Nakajima, Y. Honda, O. Kitao, H. Nakai, T. Vreven, J.A. Montgomery, J.E. Peralta, F. Ogliaro, M. Bearpark, J.J. Heyd, E. Brothers, K.N. Kudin, V.N. Staroverov, R. Kobayashi, J. Normand, K. Raghavachari, A. Rendell, J.C. Burant, S.S. Iyengar, J. Tomasi, M. Cossi, N. Rega, J.M. Millam, M. Klene, J.E. Knox, J.B. Cross, V. Bakken, C. Adamo, J. Jaramillo, R. Gomperts, R.E. Stratmann, O. Yazyev, A.J. Austin, R. Cammi, C. Pomelli, J.W. Ochterski, R.L. Martin, K. Morokuma, V.G. Zakrzewski, G.A. Voth, P. Salvador, J.J. Dannenberg, S. Dapprich, A.D. Daniels, Farkas, J.B. Foresman, J. V Ortiz, J. Cioslowski, D.J. Fox, Gaussian, Inc., Wallingford CT. (2009).

[22] (a) P.J. Hay, W.R. Wadt, *Ab initio* effective core potentials for molecular calculations.

Potentials for the transition metal atoms Sc to Hg, J. Chem. Phys. 82 (1985) 270-283. (b) https://bse.pnl.gov/bse/

[23] T. Lu, F. Chen, Multiwfn: A multifunctional wavefunction analyzer, J. Comput. Chem. 33 (2012) 580–592.

[24] (a) L. Song, Z. Chen, F. Ying, J. Song, X. Chen, P. Su, Y. Mo, Q. Zhang, W. Wu, XMVB 2.1: An ab initio non-orthogonal valence bond program, Xiamen University, Xiamen 361005, China (2015). (b) Z. Chen, F. Ying, X. Chen, J. Song, P. Su, L. Song, Y. Mo, Q. Zhang, W. Wu, XMVB 2.0: A new version of Xiamen valence bond program, Int. J. Quantum Chem. 115 (2015) 731-737. (c) L. Song, Y. Mo, Q. Zhang, W. Wu, XMVB: A program for ab initio nonorthogonal valence bond computations, J. Comput. Chem. 26 (2005) 514-521. (d) Z. Chen, X. Chen, W. Wu, Nonorthogonal orbital based N-body reduced density matrices and their applications to valence bond theory. I. Hamiltonian matrix elements between internally contracted excited valence bond wave functions, J. Chem. Phys. 138 (2013) 164119.

[25] a) P.C. Hiberty, J.P. Flament, E. Noizet, Compact and accurate valence bond functions with different orbitals for different configurations: application to the two-configuration description of $F_2$, Chem. Phys. Lett. 189 (1992) 259-265. b) P.C. Hiberty, S. Humbel, C.P. Byrman, J.H. van Lenthe, Compact valence bond functions with breathing orbitals: Application to the bond dissociation energies of $F_2$ and FH, J. Chem. Phys. 101 (1994) 5969. c) P.C. Hiberty, S. Shaik, Breathing-orbital valence bond method – A modern valence bond method that includes dynamic correlation, Theor. Chem. Acc. 108 (2002) 255-272.

[26] S. Shaik, P.C. Hiberty, A Chemist's Guide to Valence Bond Theory, Wiley, Hoboken, 2008.

[27] E.A. Rohlfing, J.J. Valentini, UV laser excited fluorescence spectroscopy of the jet-cooled copper dimer, J. Chem. Phys. 84 (1986) 6560-6566.

[28] V. Beutel, H.G. Krämer, G.L. Bhale, M. Kuhn, K. Weyers, W. Demtröder, High resolution isotope selective laser spectroscopy of $Ag_2$ molecules, J. Chem. Phys. 98 (1993) 2699-2708.

[29] M.D. Morse, Clusters of transition-metal atoms, Chem. Rev. 86 (1986) 1049-1109.

[30] B. Braida, J. Toulouse, M. Caffarel, C.J. Umrigar, Quantum Monte-Carlo with Jastrow-valence-bond wavefunctions, J. Chem. Phys. 134 (2011) 084108.

[31] H. Zhang, D. Danovich, W. Wu, B. Braida, P.C. Hiberty, Charge-shift bonding emerges as a distinct electron-pair bonding family from both valence bond and molecular orbital theories, J. Chem. Theory Comput. 10 (2014) 2410-2418.

[32] P.C. Hiberty, R. Ramozzi, L. Song, W. Wu, S. Shaik, The physical origin of large

covalent-ionic resonance energies in some two-electron bonds, Faraday Discuss. 135 (2007) 261-272.

[33] B.H. Chirgwin, C.A. Coulson, The electronic structure of conjugated systems. VI, Proc. R. Soc. London, A, 201 (1950) 196-209.

[34] W. Wu, Y. Mo, Z. Cao, Q. Zhang, A spin–free approach for valence bond theory and its applications, in: D.L. Cooper (Ed), Valence Bond Theory, Elsevier, Amsterdam, 2002; pp. 143−185.

[35] P. Anderson, A. Petit, J. Ho, M.P. Mitoraj, M.L. Coote, D. Danovich, S. Shaik, B. Braida, D.H. Ess, Protonated alcohols are examples of complete charge-shift bonds, J. Org. Chem. 79 (2014) 9998- 10001.

[36] (a) L. Song, J. Song, Y. Mo, W. Wu, An efficient algorithm for energy gradients and orbital optimization in valence bond theory, J. Comput. Chem. 30 (2009) 399-406. (b) Z. Chen, X. Chen, W. Wu, Nonorthogonal orbital based *N*-body reduced density matrices and their applications to valence bond theory. II. An efficient algorithm for matrix elements and analytical energy gradients in VBSCF method, J. Chem. Phys. 138 (2013) 164120 (c) X. Chen, Z. Chen, W. Wu, Nonorthogonal orbital based *N*-body reduced density matrices and their applications to valence bond theory. IV. The automatic implementation of the Hessian based VBSCF method, J. Chem. Phys. 141 (2014) 194113 (d) Z. Chen, C. Zhou, W. Wu, Seniority number in valence bond theory, J. Chem. Theory Comput. 11 (2015) 4102-4108.

**Table 1.** Bond dissociation energies, in kcal/mol, at different level of VB theory, together with CCSD(T) values in the same basis set (see computational details) and experimental values for reference.

| | $Cu_2$ | $Ag_2$ | $Au_2$ |
|---|---|---|---|
| L-VBSCF (**1-3**) | 15.0 | 15.6 | 20.0 |
| L-VBSCF (**1-9**) | 22.2 | 19.3 | 23.9 |
| L-BOVB (**1-9**) | 26.7 | 24.1 | 37.6 |
| SL-BOVB (**1-9**) | 32.7 | 26.3 | 39.6 |
| SD-BOVB (**1-9**) | 40.7 | 28.9 | 47.4 |
| CCSD(T) | 40.5 | 33.3 | 48.5 |
| experimental | 47.7[a] | 38.3[b] | 52.8[c] |

[a] Reference [27] ; [b] Reference [28]; [c] Reference [29]

**Table 2.** SD-BOVB weights of the structures **1-9** in the studied coinage metal dimers (Fig. 1).

| | $Cu_2$ | $Ag_2$ | $Au_2$ |
|---|---|---|---|
| **1** | 0.714 | 0.612 | 0.400 |
| **2+3** | 0.258 | 0.358 | 0.586 |
| **4+5** | 0.008 | 0.010 | 0.010 |
| **6–9** | 0.020 | 0.020 | 0.004 |

**Table 3.** VB and AIM bond properties characteristic of the nature of bonding in homoatomic dimers. The $D_{cov}$ is the covalent bond dissociation energy (see text), BDE the total bond dissociation energy, $RE_{CS}$ the "charge-shift resonance energy" (see text), all computed at the SD-BOVB level, and expressed in kcal/mol. %RE correspond to the perscentage of the total BDE that the $RE_{CS}$ represents. The last two columns display AIM related quantities: $\rho(r_c)$ the electron density at the bond critical point, and $\nabla^2(r_c)$ the Laplacian of the density at the bond critical point.

| | $D_{cov}$ | BDE | $RE_{CS}$ | %RE | $\rho(r_c)$ | $\nabla^2\rho(r_c)$ |
|---|---|---|---|---|---|---|
| $Cu_2$ | 20.9 | 40.7 | 19.7 | 48.5 | 0.04 | +0.13 |
| $Ag_2$ | 17.6 | 28.9 | 11.3 | 39.2 | 0.04 | +0.16 |
| $Au_2$ | 23.0 | 47.4 | 24.4 | 51.5 | 0.08 | +0.19 |
| $F_2$ | -40.9 | 37.6 | 78.4 | 208.8 | 0.32 | +0.20 |
| $Li_2$ | 19.1 | 23.6 | 4.4 | 18.7 | 0.01 | -0.01 |
| $H_2$ | 99.4 | 106.9 | 7.6 | 7.1 | 0.27 | -1.23 |

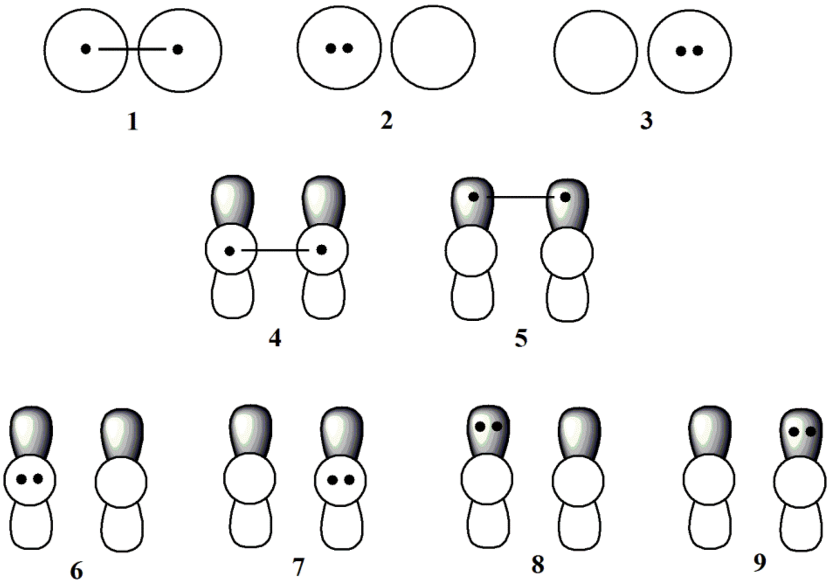

**Figure 1.** VB basis of structures for the 2c/2e bond of the coinage metal dimers.

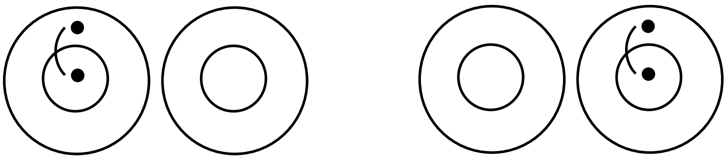

**2'** **3'**

**Figure 2.** Schematic representation of the active orbital splitting in the main ionic structures at the SL-BOVB level. The dots represent the two electrons of the 4s-type pair, and the curve connection the dots indicate a singlet coupling between the two electrons in the two split orbitals 2a and 2b (resp. 3a and 3b) in structure **2’** (resp. **3’**).

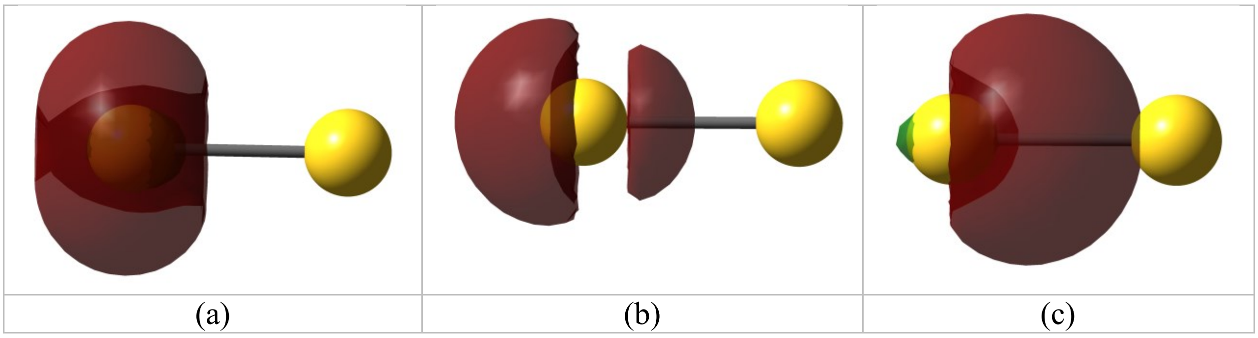

(a) (b) (c)

**Figure 3.** Computed 4s-type VB orbitals of $Au_2$ at the SL-BOVB level, (a): in the covalent structure **1**, and (b) and (c): the “split” pairs of orbitals in the ionic structure **2’** (see Figure 2 for a schematic representation of this VB structure).

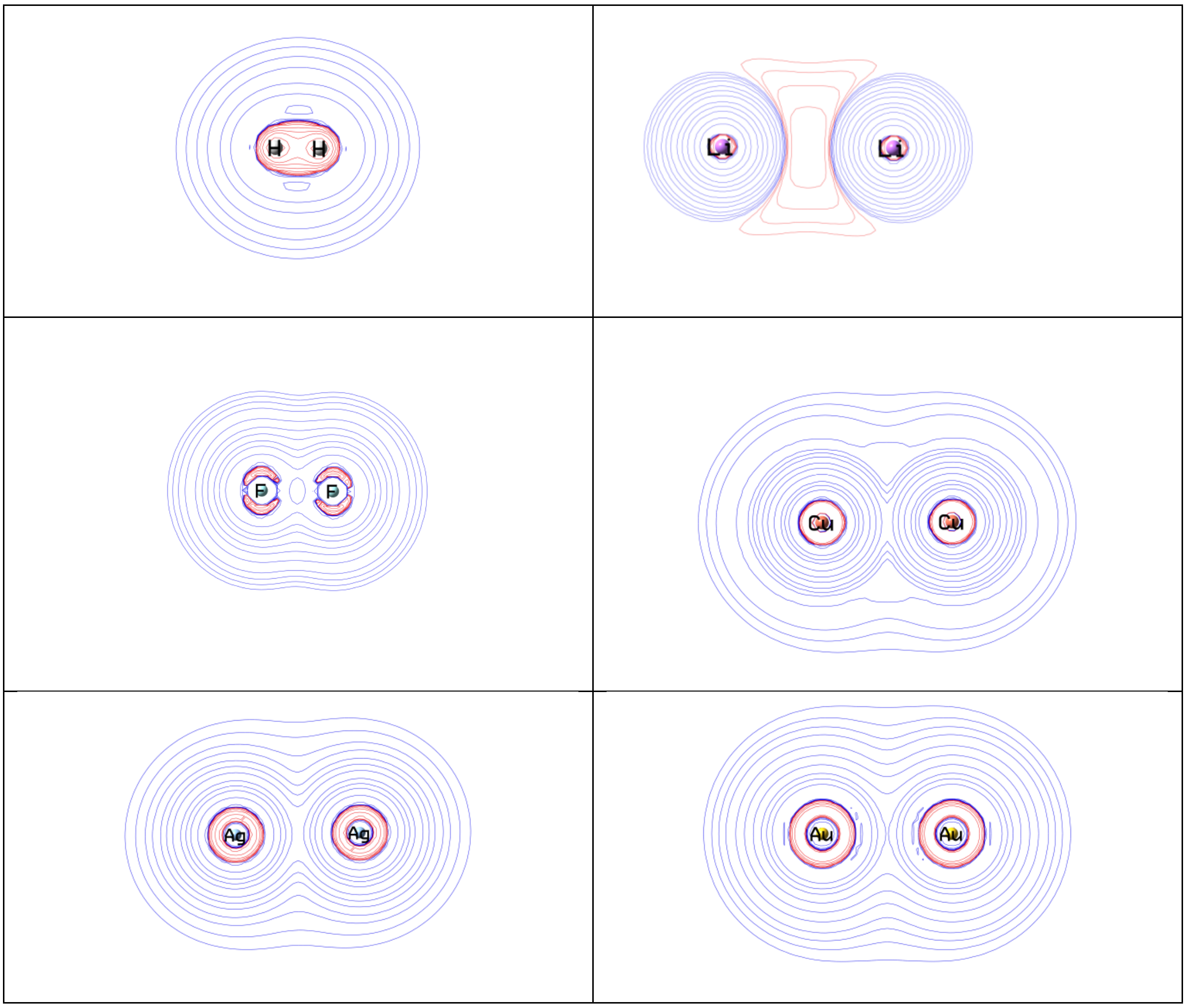

**Figure 4.** Distribution of $\nabla^2\rho$ in the xz-plane (atoms lay along the z-axis). Blue lines indicate areas of charge depletion (positive values of $\nabla^2\rho$) and red lines indicate areas of charge concentration (negative values of $\nabla^2\rho$). The $H_2$ and $Li_2$ molecules (top left and right drawings respectively) provides example of covalent bonding, while $F_2$ (middle left) provides an example of complete Charge Shift Bond. The coinage metal dimers correspond to middle right ($Cu_2$), bottom left ($Ag_2$) and bottom right ($Au_2$) figures.